Illuminating Quantum Magnetic Gases: Constructing a Rotating Waveplate Polarimeter

Thomas Huckans – thh2@williams.edu

Project Mentor: Benjamin Pasquiou – benjamin.pasquiou@univ-paris13.fr

Laboratoire de Physique des Lasers

June 5th – July 28th, 2023

Table of Contents

Abstract

In the scientific community's efforts to better understand quantum mechanics, the study of ultracold gases has proven quite fruitful. After the gases are cooled to temperatures in the range of just several nanokelvin, otherwise impossible-to-detect interactions are revealed. I undertook my project in the Magnetic Quantum Gases group, which is presently conducting two experiments making use of strontium-87, one of them being the construction of a continuous superradiant laser. When performing research with the aid of lasers and other optical elements, knowing the polarization of the light is a necessity. However, polarimeters are typically very expensive or inconvenient to use. Thus, the in-house construction of a portable rotating waveplate polarimeter would address both of those problems, aiding in the development of the superradiant laser experiment. For the first iteration built, the rotating waveplate polarimeter is capable of measuring variations in the intensity of light to create a Poincaré sphere indicating the light's polarization. For future work, we would like to shrink the overall size of the device, allowing it to be placed in smaller areas on an optical table, without potentially damaging or misaligning optics. In addition, an enclosure could be added to reduce the noise created by the polarimeter, which could interfere with delicate alignments and data taking.

Acknowledgments

Before I begin, I would be remiss to not express my deep gratitude to a number of individuals, without whom this internship would not have been possible. Foremost, I owe much to my advisor, mentor, and internship liaison, Benjamin Pasquiou, and to Bruno Laburthe-Tolra, Martin Robert de Saint Vincent, and the entire Magnetic Quantum Gases (GQM) team at the Laboratoire de Physique des Lasers (LPL). Not to be forgotten, the mechanical shop experts Mathieu Goncalves and Albert Kaladjian were invaluable in the design and construction of the rotating waveplate polarimeter.

Next, I have deep gratitude for the mentorship and education I received from Professors Katharine Jensen and Protik Majumder, and for Professor Jensen for both encouraging me to do research abroad and acting as my representative to the Centre National de la Recherche Scientifique (CNRS). Moreover, I could never thank my father, John Huckans, enough for being my biggest inspiration and supporter in all my endeavors. Without his guidance, help, and love, none of this could have happened.

Thank you also to the friends and family of both Collin Roche and Lilli Gomez, as without their generous funding of my fellowship, none of my experiences would have been anything more than dreams. In that same vein, a warm thanks to Dr. Katya King and all those at the Williams Office of Fellowships for their tireless work in supporting students.

Introduction

In today's research, lasers are ubiquitous in experiments ranging from metallurgy to biophysics to quantum physics. However, an important practical problem lies in how to achieve the necessary precision for many of these experiments studying fundamental physical concepts. Currently, the most stable lasers in the world are used in the most precise of atomic clocks, achieving frequencies of emission stable to eighteen decimal places. Unfortunately, these lasers are expensive to build, require monumental efforts to stabilize them, and perform poorly outside of a lab, leading to a situation where only the best funded labs have access to those levels of precision.[1] Superradiance can change that.

In a typical laser, light in a cavity is bounced back and forth by two mirrors through a light-emitting material, and then a small portion of light (the laser beam) is allowed to escape into a second stabilization cavity. The problem lies in fluctuations in the length of the second cavity, which leads to elaborate and expensive engineering in ultra-precise lasers. In a superradiant laser, the laser's stability does not depend on a second stabilization cavity, and only uses a primary cavity. Instead, the light-emission material is superradiant—a densely-packed cloud of cold atoms that emit ultra-narrow linewidth light as they transition from one energy eigenstate to a lower one. The goal is that these superradiant lasers will make high-precision research available to many more members of the scientific community. To be clear, superradiance was first achieved in 2012, but in a discontinuous, pulsed form.[2] To use these lasers more effectively, the Gaz Quantiques Magnétiques (GQM) team at the Laboratoire de Physique des Lasers (LPL) and a handful of other teams around the world are diligently working to build continuous superradiant lasers.

---

[1] Liu, H. et al., (2020).
[2] Bohnet, J. G. et al., (2012)

When experiments require such high precision, measuring whether light is linearly, circularly, or elliptically polarized is paramount. For instance, circularly polarized light elicits different reactions from certain materials, and can also influence which spin states an atom enters. Linearly polarized light is important for many types of experiments, particularly when transmitting the light through polarization-maintaining optical fibers, which require specific linear orientations. The rotating waveplate polarimeter thus makes the acquisition of information much more efficient, as it is both inexpensive when compared to typical tools and faster than trying to deduce the polarization via trial and error. Specifically, the GQM team is interested in investigating the effects of the collective spontaneous emission phenomenon, superradiance, such as the spontaneous emergence of entanglement and altered emission properties.[3]

Principles and Methods

Quarter waveplates, specifically ones that rotate, give our polarimeter its ability to polarize light. As is well known, whenever light passes through a medium, it picks up a phase, where $E_{out}=E_{in}e^{(-i*n*k*d)}$, where E is the amplitude of the light's electric field, n is the medium's index of refraction, k the wavenumber of the light, and d the length of the medium through which the beam propagates.[4]

For my project, I used a quarter waveplate, which can transform linearly polarized light to circular, and vice versa, depending on the angle between the polarization axes of the crystal and the light.[5] If the light's polarization is linear, there are four angles at which it is transformed into circular, and if circular, there are two angles at which it is transformed into linear. By

[3] Robert-de-Saint-Vincent, M., Pasquiou, B., Laburthe-Tolra, B. (2021)
[4] Zambrana-Puyalto, X. (2020)
[5] Lu, S., & Loeber, A. P. (1975)

rotating the waveplate rapidly at a frequency *f* and then Fourier transforming the polarizing beam splitter (PBS)-analyzed output, one sees maxima at either 4*f* or 2*f* depending on whether the light is linearly or circularly polarized, respectively. If both frequencies are observed at varying magnitudes, then the light is a combination of the two that is related to the magnitudes calculated by the Fast Fourier Transform (FFT). In the rotating waveplate polarimeter, a photodiode is used to collect the fluctuating intensity of the light coming from PBS analyzer, and the signal is measured by an oscilloscope. Afterwards, the amplitudes of the signal's frequencies can be calculated by a computer performing the FFT.

We created a model of the physics on Wolfram's Mathematica, simulating the effects of variable polarizations of light passing through a rotating quarter waveplate. The graphs displayed in Figs. 1 and 2 employ a relative scale of the intensity of light, depending on the type of waveplate used (half or quarter) as well as the initial polarization of the incoming light. For the second slider in the figures, ε is the initial phase shift of the y-axis component of the traveling electromagnetic wave, changing the simulated light's polarization. An ε value of 0, 0.5, or 1 is circular, whereas 0.25 and 0.75 are linear. For the first slider, x is the type of waveplate used, where a value of 4 represents a quarter waveplate and a 2 a half waveplate.

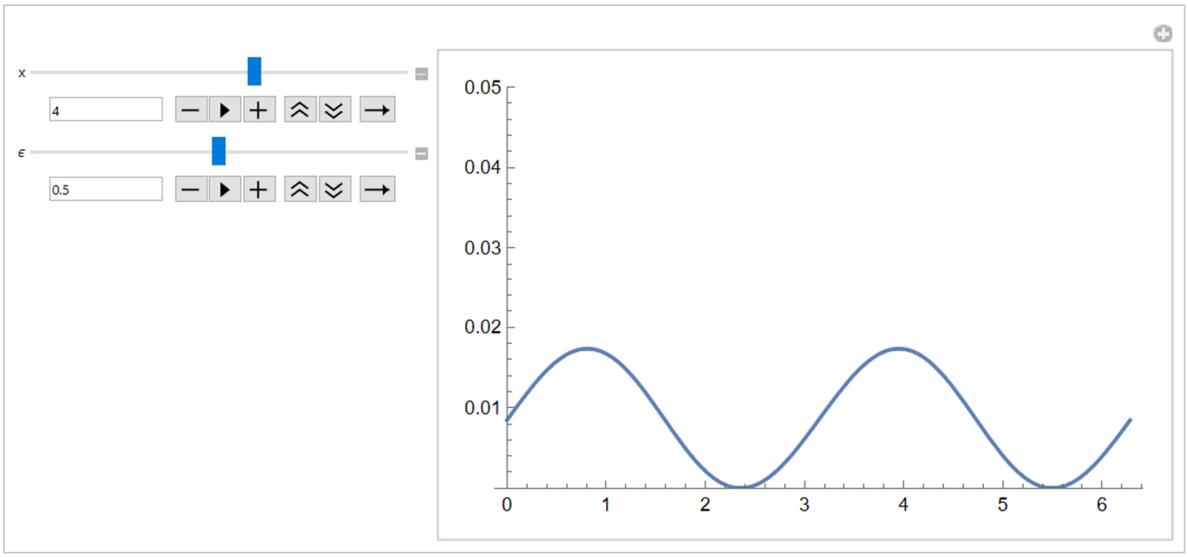

FIG. 1: Visual representation of time-varying signal for circularly polarized light. As the model shows, in one full rotation of the waveplate there are two maxima of light intensity.

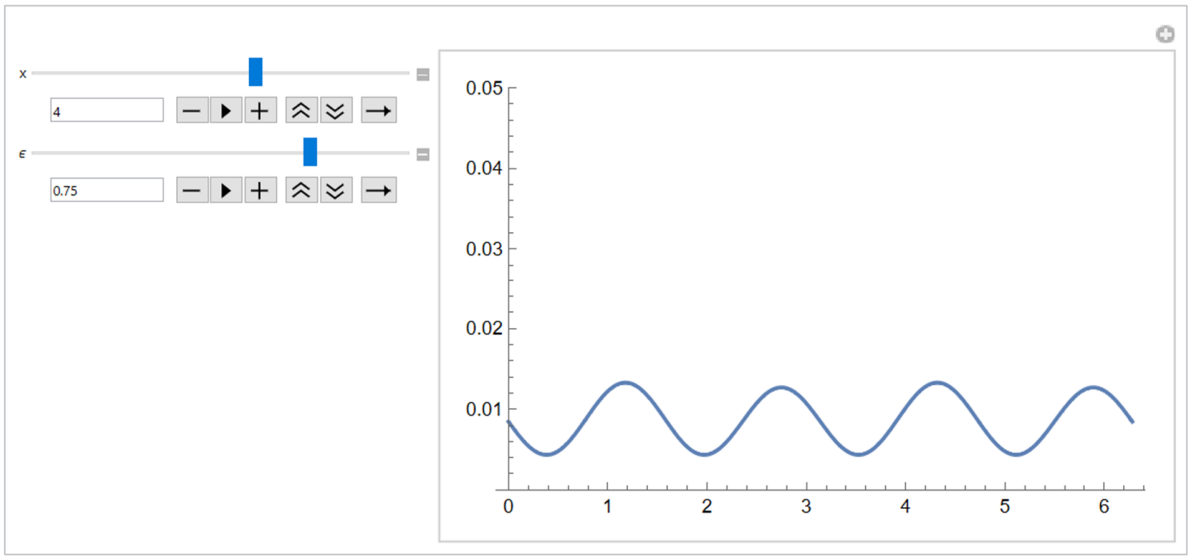

FIG. 2: Visual representation of time-varying signal for linearly polarized light. As the model shows, in one full rotation of the waveplate there are four maxima of light intensity.

The phenomenon of multiple peaks is demonstrated clearly by the number of maximum intensities of light in the 2π periods modeled for either a quarter or half waveplate; pertinent code can be found in Appendix A.

Construction

Design

After an initial failed attempt with a discarded computer hard drive motor, we decided to use a DC brush motor, which had much higher torque capabilities. The motor could then connect to a pulley gear and a timing belt, which would connect to a second pulley gear inserted over a lens tube that held the waveplate inside. We used SolidWorks to design the gears and went through several iterations before finding the correct match to the belt already owned by the lab. In the initial design, the lens tube was inserted within two large ball bearings, so that the tube rotated internally. Unfortunately, the large bearings had too much friction, and the scavenged parts used to support the bearings were insufficient, so a second design had to be created.

To measure the rotational speed of the waveplate, we decided to insert magnets in the gear containing the lens tube and therefore use changes in the magnetic field to know when each rotation was completed. Using a Hall probe, we measured the changing magnetic field as the gears spun, and then transformed the analog signal into a digital one using a TTL logic gate—a Schmitt trigger, instead of a varying analog signal prone to jitter noise. If the conditions specified by the logic gate were met (magnetic field sensed), then it gave a 5 V true Boolean, which was more easily analyzable. The reason being is that the spectrum of the Hall probe's analog signal is prone to variation and more inherently complicated; moreover, the addition of a logic gate amplifies our signal from 1 V to 5 V, thus improving our signal-to-noise ratio.

The second iteration (Cradle 2.0) removed the friction problems by using smaller, smoother ball bearings, upon which the lens tube rested. We wanted the cradle to be one part,

and rather than ordering or finding parts to cobble together, the Cradle 2.0 was fabricated entirely in-house by the mechanical workshop.

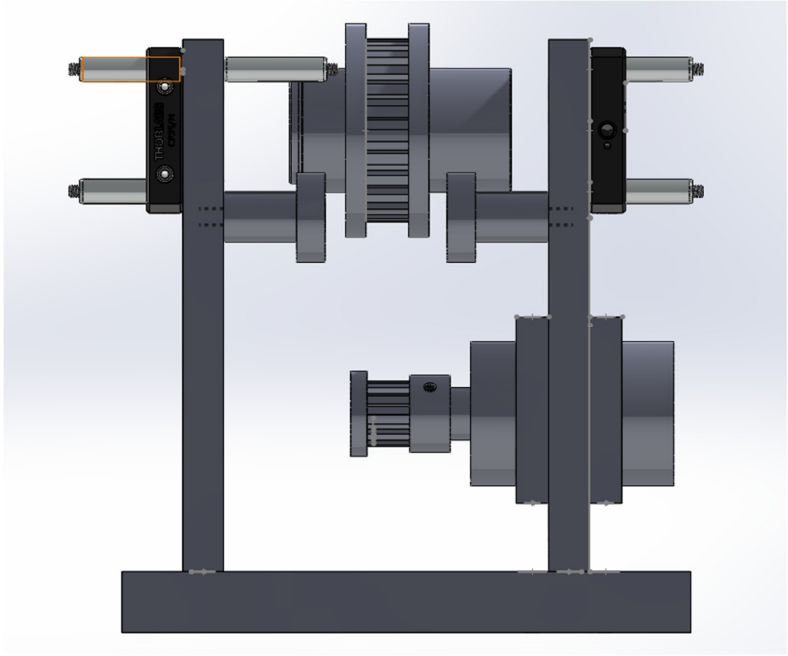

FIG. 3: Orthographic view of the Cradle 2.0 depicting the lens tube resting upon ball bearings and the DC motor fastened below it.

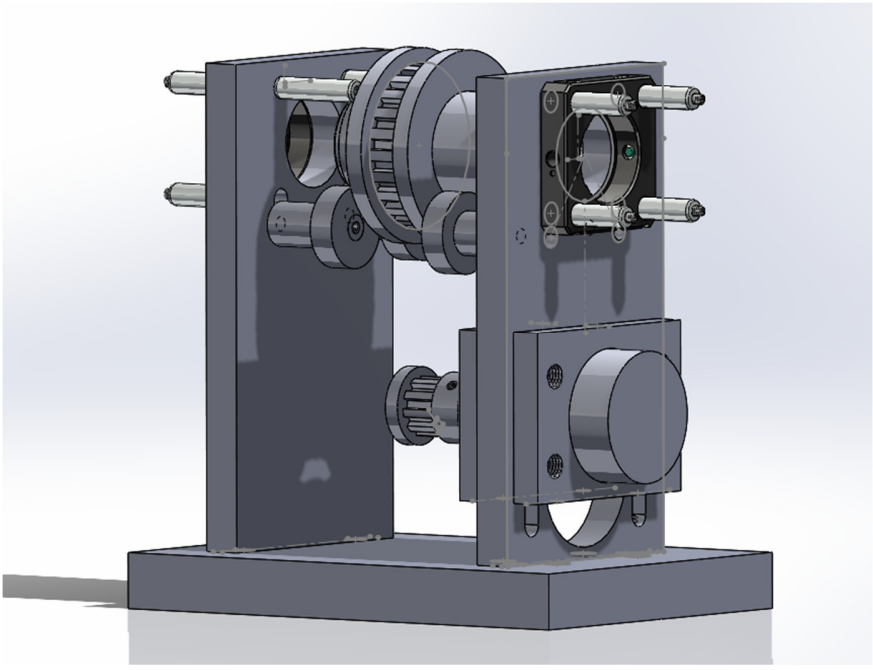

FIG. 4: Isometric view of the Cradle 2.0 showing how the DC motor is attached to the cradle and an alternate view of how the lens tube is supported.

Characterization

The photodiode used for the polarimeter has part number UDT455HS, manufactured by OSI Optoelectronics, with a sensitivity of 1 V per 0.093 mW of captured light power at 654 nm. It is powered with ±15 V and must be used with its dedicated AC/DC converter. Only 600 Hz bandwidth is required of the photodiode, since our DC brush motor should not rotate faster than 9,000 rpm, or 150 Hz. The maximum peak frequency of linear light that we expect to see is four times this rotation rate, thus 600 Hz.

A standard oscilloscope was used to measure the photodiode maximum bandwidth. Using the trigger feature of the oscilloscope, a flashlight was quickly turned on and off, so the exponential decay of the capacitors within the photodiode could be measured. As shown in Fig. 5, approximately 14 μs after the light was turned off, 95% of the signal had decayed, with an approximate uncertainty of 2 μs. Using the time constant formula ($\tau = 1 / (2\pi * f)$, where f is the frequency and 3τ is equal to 14 μs), we found the maximum frequency to be 34 kHz ± 5 kHz. Clearly, the photodiode is more than sufficient for the role it plays in the polarimeter.

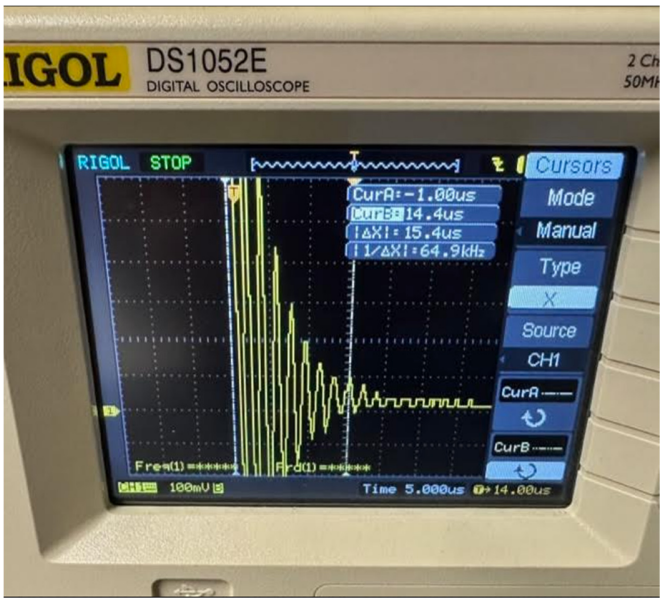

FIG. 5: Characterization of photodiode, revealing a maximum frequency of 33 kHz ± 4.4 kHz. As seen, 95% of the signal decayed in about 14 μs (±2 μs).

Implementation

In order to power the polarimeter, a variable voltage and current power supply was attached to the DC motor, which allowed for testing of the polarimeter's upper and lower working ranges. Ideal ranges were found to be no less than 1 V and between 9 to 10 A. In addition, light was drawn from the 654 nm laser used in the chromium experiment to test the polarimeter. We began a lengthy injection and alignment process into a polarization-maintaining fiber, but in the end, we only obtained 29% injection efficiency (210 μW out of 725 μW). Fortunately, efficiency was not a large concern, as the power of the beam mattered significantly less than its ability to be manipulated.

Then, with the Cradle 2.0 fully assembled, it was evaluated by polarizing the 654 nm light to be linear, circular, or elliptical. We saw that the magnitudes of intensity peaks corresponded well to the polarization of the 654 nm light it was receiving, and the spinning tube containing the quarter waveplate provided swift analysis of the incoming beam.

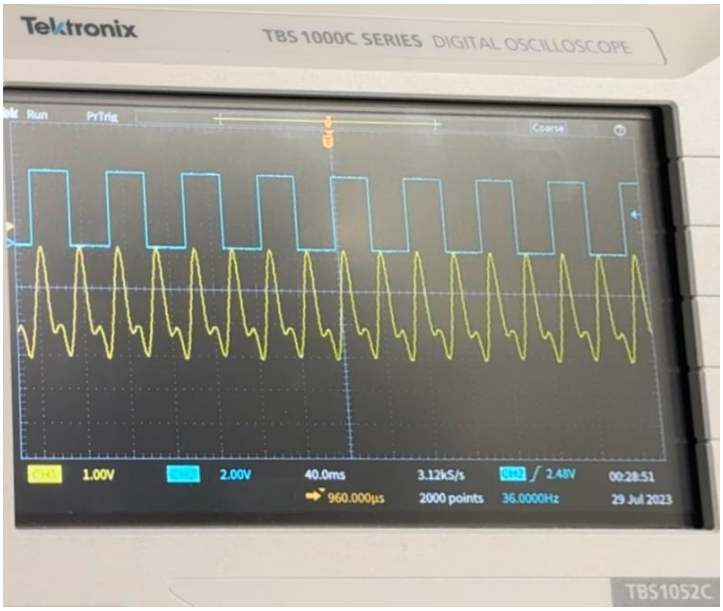

FIG. 6: View of the signals from the Schmitt trigger with the Hall monitor (blue) and the photodiode (yellow). In this case, the incoming light is elliptically polarized, but with a greater percentage of circular than linear polarization.

The code developed, under significant direction and guidance from Dr. Pasquiou, is written in Python, and imports data from an oscilloscope, either real-time or saved, analyzes the Stokes parameters of the fluctuating light, and then creates a Poincaré sphere that pictorially represents the polarization of any received light. It has an interactive graphical user interface (GUI) and is quick to compile and process.

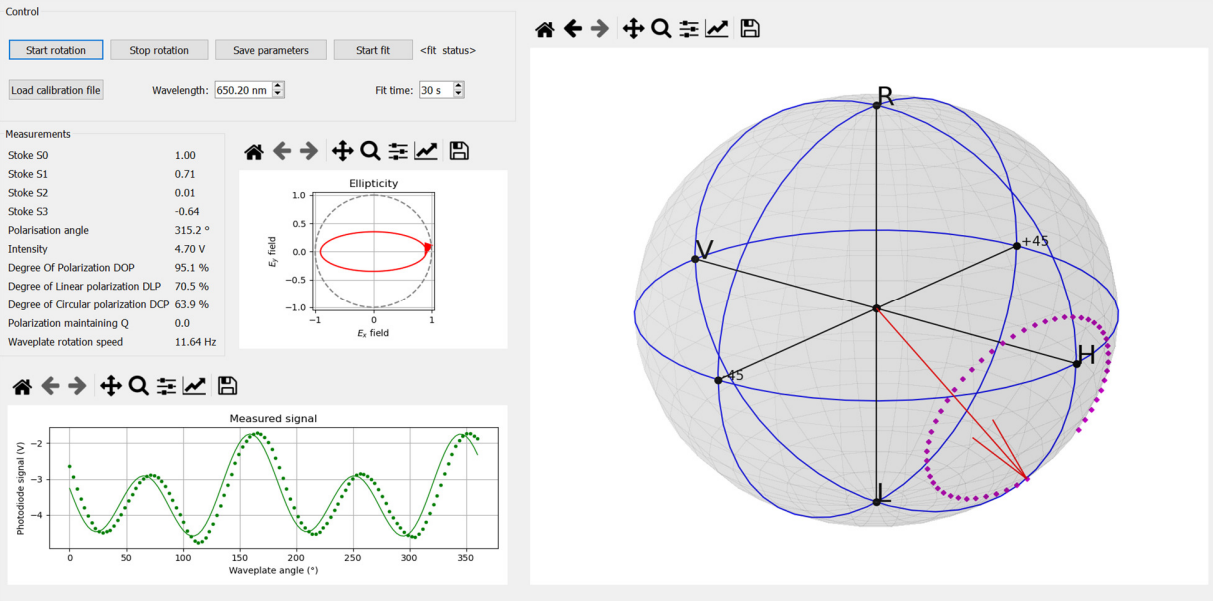

FIG. 7: Finished code for Poincaré sphere and Stokes parameters. The terminal displays the photodiode signal, ellipticity, various parameters of the waveplate, polarization, and Stokes parameters, and the Poincaré sphere's arrow displays changing polarization as the waveplate rotates.

User Guide

In its current setup, the rotating waveplate polarimeter needs power for three components: the DC brush motor, the photodiode, and the Hall probe circuit. The photodiode requires a ±15 V DC power source, the Hall probe functions at a minimum of 4.5 V DC, but the DC brush motor requires greater specificity. We found that its minimum requirements to run were 1 V and 8.5 A, to ensure steady rotation. However, the best range at which to use the polarimeter is from 9 to 10 A and 1.1 to 1.2 V.

The lens tube typically requires a gentle nudge to begin its rotation, which should be corrected in a future design. To measure the data, the current iteration requires connecting an oscilloscope to both the Hall probe and the photodiode, and then downloading that data onto a computer, where a script analyzes and displays the light's polarization. Finding the period of rotation using the Hall probe is simpler than finding the period of the photodiode signal, as an FFT of a square wave has a smaller spectrum of variation.

Finally, the height of the DC brush motor can be adjusted, which enables greater stability and gives a wider range of options for which the same timing belt can be used. To be most effective, the screws that change the vertical position of the DC motor should be tightened so that there is some tension in the timing belt, but it is not completely taut.

Conclusion

The purpose of the rotating waveplate polarimeter was clear: provide an economical, easy-to-use alternative to the costly polarimeters employed by most labs. At manufacturers such as Thorlabs, a polarimeter can cost more than 6,000USD, which can be extraordinarily straining to a lab's budget. This polarimeter was constructed almost entirely in-house, ordering only timing belts to connect the DC motor to the tub and ball bearings to enable it to turn. Everything else was constructed or recycled in-house, such as the 3D printed gears, the machined body of the Cradle 2.0, a repurposed DC brush motor and a found lens tube. The total cost was a tiny fraction of a commercial polarimeter, and after further modifications and improvements, could perform nearly identically.

Of course, commercial polarimeters are much smaller, which is useful when trying to fit them into densely packed optics tables or in tightly crammed experiments. Although the

spinning quarter waveplate sets a certain minimum threshold of size, the overall design of the cradle could be shrunk considerably by decreasing the length of the lens tube, moving the DC brush motor closer to the tube, and integrating the photodiode more carefully into the piece. This would allow for a smaller chassis and a more efficient use of space, enabling greater use of the polarimeter.

In addition, when the polarimeter rotates, it creates a noise that is significant enough to potentially disrupt an alignment or affect an experiment it is being used on. To combat this, a preliminary step could be the creation of a plexiglass enclosure of the metal body, which would mute the sound. In addition, the noise comes from the spinning of the lens tube on the ball bearings, and future iterations could incorporate frictionless or friction-reducing components.

Appendix

Mathematica code for model of fluctuating light intensity, which created figures 1 and 2.

```
"BEGINNING OF PERTINENT CODE
  t is the period of the electromagentic signal
  ω is the rotation frequency of the waveplate
  ϵ is the intial phase shift of one of the axes of the light
     (changes the intial polarization)
  x is the type of wave plate (one would select 4 for a λ/4 waveplate)"
Ex[t_, ϵ_] := Cos[t + π / 2 + 2 π * ϵ]
Ey[t_, ϵ_] := Cos[t]

EX[ω_, t_, ϵ_] := Cos[ω] * Ex[t, ϵ] + Sin[ω] * Ey[t, ϵ]
EY[ω_, t_, ϵ_] := -Sin[ω] * Ex[t, ϵ] + Cos[ω] * Ey[t, ϵ]

EXX[ω_, t_, ϵ_] := EX[ω, t, ϵ]
EYY[ω_, t_, ϵ_, x_] := EY[ω, t - 2 * π * 1 / x, ϵ]

EXXX[ω_, t_, ϵ_, x_] := Cos[-ω] * EXX[ω, t, ϵ] + Sin[-ω] * EYY[ω, t, ϵ, x]
EYYY[ω_, t_, ϵ_, x_] := -Sin[-ω] * EXX[ω, t, ϵ] + Cos[-ω] * EYY[ω, t, ϵ, x]
"Intensity of Light,depending on waveplate and inital polarization
-ϵ is the intial phase shift of one of the axes of the light
   (changes the intial polarization, where 0, 0.5 and 1 are perfectly
    circular and 0.25 and 0.75 are linear)
-x is the type of wave plate (one would select 4 for a λ/4 waveplate) "
Intensity[ω_, ϵ_, x_] = 3 * 10^8 * 8.854 * 10^-12 * Sum[EYYY[ω, t, ϵ, x]^2,
     {t, 0, 2π, (2π / 40)}] / (2π);
Manipulate[Plot[Intensity[ω, ϵ, x], {ω, 0, 2π}, PlotRange → {0, 0.05}],
 {x, 1, 6}, {ϵ, 0, 1}]|
```

Table setup of the rotating waveplate polarimeter.

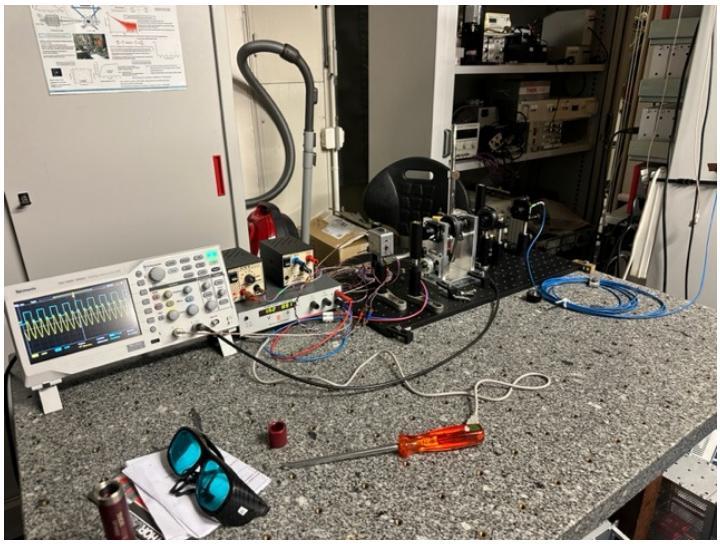

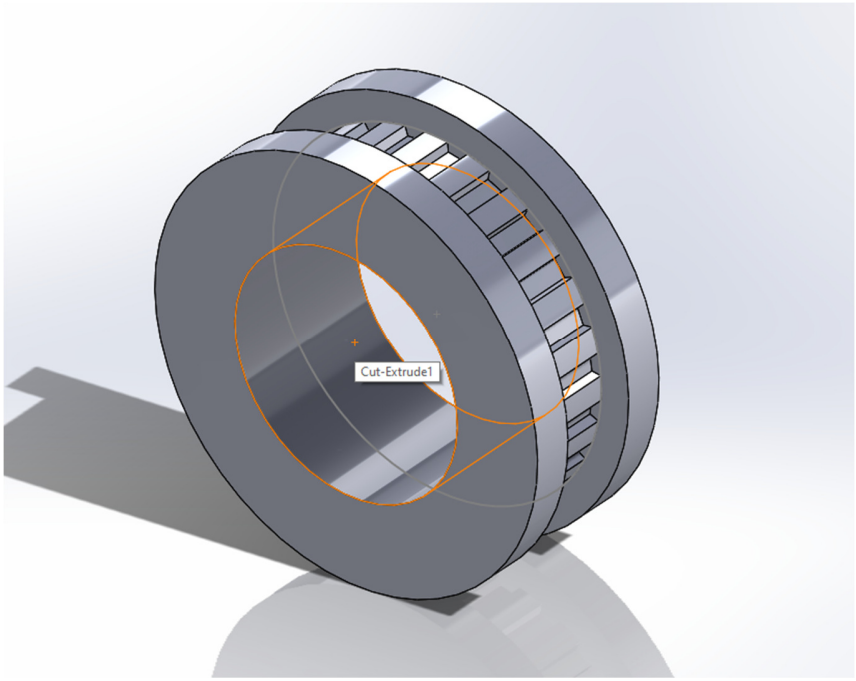

Big pulley gear: inserted around lens tube.

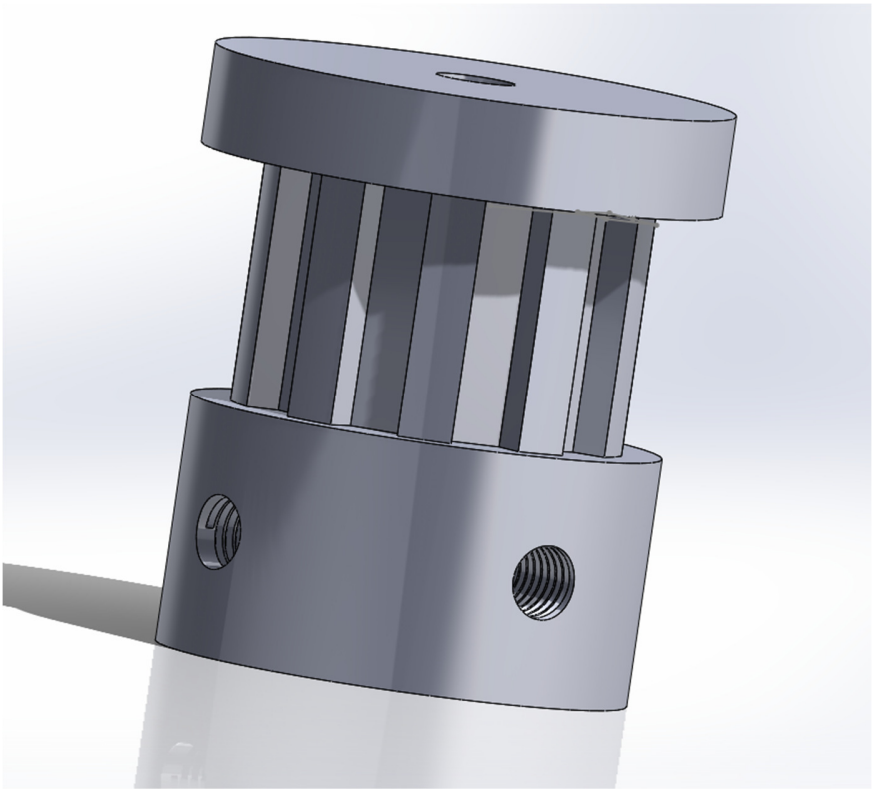

Small pulley gear: attached to DC brush motor.

Bibliography

Bohnet, J. G., Chen, Z., Weiner, J. M., Meiser, D., Holland, M. J., & Thompson, J. K. (2012). A steady-state superradiant laser with less than one intracavity photon. Nature, 484(7392), 78–81. https://doi.org/10.1038/nature10920

Liu, H., Jäger, S. B., Yu, X., Touzard, S., Shankar, A., Holland, M. J., & Nicholson, T. L. (2020). Rugged Mhz-linewidth superradiant laser driven by a hot atomic beam. *Physical Review Letters*, *125*(25). https://doi.org/10.1103/physrevlett.125.253602

Lu, S., & Loeber, A. P. (1975). Depolarization of white light by a birefringent crystal. *Journal of the Optical Society of America*, *65*(3), 248. https://doi.org/10.1364/josa.65.000248

Robert-de-Saint-Vincent, M., Pasquiou, B., Laburthe-Tolra, B. (2021). The super-radiant laser project. Cold atoms Group, Laboratoire de Physique des Lasers. https://gqm.lpl.univ-paris13.fr/AF/SuperRadiantLaserProject.htm

Wolfram Research, Inc., Mathematica, Version 13.3, Champaign, IL (2023).

Zambrana-Puyalto, X. (2020). Waveplates: Physical principles, uses and purchase tips. Photoniques, (104), 53–57. https://doi.org/10.1051/photon/202010453